On the Effects of Parameter Adjustment on the Performance of PSO-Based MPPT of a PV-Energy Generation System

André Luiz Marques Leopoldino(✉), Cleiton Magalhães Freitas, and Luís Fernando Corrêa Monteiro

Rio de Janeiro State University, Rio de Janeiro, Brazil
andre.leopoldino@gmail.com, {cleiton.freitas,lmonteiro}@uerj.br

Abstract. The growing concern on environmental issues caused by fossil fuels and, indeed, on the availability of such energy resources in a long-run basis have settled the ground for the spreading of the so called green energy sources. Among them, photovoltaic energy stands out due to the possibility of turning practically any household into a micro power plant. One important aspect about this source of energy is that practical photovoltaic generators are equipped with maximum power point tracking (MPPT) systems. Currently, researchers are focused on developing MPPT algorithms for partial shaded panels, among which, particle swarm optimization (PSO) MPPT stands out. PSO is an artificial intelligence method based on the behavior of flock of birds and it works arranging a group of mathematical entities named particles to deal with an optimization problem. Thus, this work focus on analyzing the performance of this algorithm under different design conditions, which means different amount of particles and different set points for the constants. Besides that, the article presents a brief guideline on how to implement PSO-MPPT. Simulations of an array with three photovoltaic panels, boost-converter driven, were carried out in order to back the analyzes.

Keywords: Photovoltaic energy generation · Maximum power point tracking · Particle swarm optimization

1 Introduction

The growing concern on environmental issues caused by fossil fuels and, indeed, on the availability of such energy resources in a long-run basis have settled the ground for the spreading of the so called green energy sources. Among them, photovoltaic (PV) energy stands out due to the possibility of turning practically any household into a micro power plant [11]. In views of that, countries such as Germany, China and Japan have taken the lead, powered either from environmental or commercial aims, of the movement of solar photovoltaic energy spreading [1,20].

J. L. Afonso et al. (Eds.): GreeNets 2018, LNICST 269, pp. 175–192, 2019.
https://doi.org/10.1007/978-3-030-12950-7_14

From the technical point of view, it is important to highlight that, in addition to PV panels, electronic converters, and others hardware components, PV-based power generation systems should be equipped with Maximum Power Point Tracking (MPPT) controllers, otherwise they may not extract the maximum amount of energy from the panel. In fact, the lack of such controllers can even turn the effective power generation impracticable. In short, the amount of power harvested from a panel depends on the voltage in the terminal of the panel itself and this relationship varies with environmental variables such as solar radiance and temperature. Thus, MPPT controllers act searching in real time for the voltage which may lead to the Maximum Power Point (MPP) of the panel. It is worthwhile noticing that methods such as Perturb and Observe (P&O), Hill Climbing, Incremental Conductance, and plenty of others based in artificial intelligence have already been extensively tested, and are considered to be reliable for this purpose [2,9,15]. Nonetheless, these methods are prone to fail in face of partial shading of the panel, situation in which the panel might present multiple maximum power points.

Regarding the operation under partial shading, a couple of other methods have already been proposed for MPPT [10], among which Particle Swarm Optimization (PSO) [7]. This method belongs to the Artificial Intelligence (AI) branch and is based on the behavior of flock of animals. Its characteristic make it possible to search for the global MPP (GMPP) without being trapped into local maxima, which would possible reduce the amount of energy harvested. A brief review of the literature shows that researchers have widely used different forms of PSO algorithms in different configurations of PV generation systems. Some authors have used PSO-MPPT for reducing steady-state oscillations [5] in a single-converter system, while other have developed algorithms for multi-converter distributed systems [14]. Besides that, it is also found in the literature PSO-MPPT applied to grid-tied systems [13]. Furthermore, some researchers have combined PSO with other techniques [8] or modified the basic concept of PSO with intention to cut off the random characteristic of the algorithm [16]. Although some authors have analyzed the influence of some parameters, such as number of particles used in the MPPT, it lacks a full analyze of the influence of the algorithm settings into the performance of the PSO-MPPT. In views of that, this work aims at analyzing how the number of particles and the tuning of constants used in a PSO algorithm affect the performance of MPPT of an array of partially shaded PV panels. In short, the performance of the PSO-MPPT was analyzed through simulation for different number of particles and settings for the constants. For this matter, it was considered a system comprised of an array of three series-connected panels, a boost converter and a 96 V battery. Apart from these analyses, it is also in the scope of this article to present a detailed description of the PSO-MPPT used in the simulations.

This work is organized in seven sections as follows: The Sect. 2 presents a review on how PV panel is modeled and the effects of the partial shading on the power $\times$ voltage (P-V) relationship. Section 3 aims at presenting the scenario proposed for analysis. After that, an introductory discussion on PSO algorithm

is carried out in Sect. 4 and, in the sequence, the PSO-MPPT algorithm analyzed in this work is detailed in Sect. 5. Section 6 presents the methodology used for analysis along with the simulation results. Finally, conclusions are drawn in Sect. 7.

2 Photovoltaic Panels

This section aims at depicting the mathematical model used for representing the PV panels, along with describing its behavior under different radiance and temperature levels. Besides that, it is also explained the effects of partial shading on the P-V curve.

2.1 PV Panel Modeling

The single diode model approach [19] was used to represent the PV panel in the simulation environment. With this model, the PV panel is represented by current source, I_{ph}, paralleled with direct biased diode and a shunt resistor, R_{sh}, as it is presented in Fig. 1. Besides that, a series resistor, R_s, is inserted in the circuital model so as to modeling the conduction losses of the panel. As the shunt resistance tends to assume high values [3], the current flowing out of the PV panel may be expressed by:

$$I_{pv} = I_{ph} - I_d \tag{1}$$

where I_d is the current flowing through the diode.

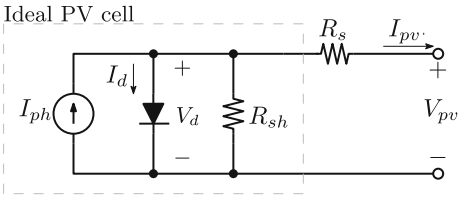

Fig. 1. Single-diode equivalent circuit of a photovoltaic cell

Basically, the current source I_{ph} model the panel response to solar irradiation and, of course, the effect of temperature on the power generation. Thus, this current can be represented as:

$$I_{ph} = \frac{G}{G_{ref}} I_{sc,ref} + C_T \left(T - T_{ref}\right) \tag{2}$$

where G and T are, respectively, the radiance in W/m^2 and temperature in K which the panel is submitted, whereas G_{ref} and T_{ref} are the reference values of

these variables for which the short-circuit current $I_{sc,ref}$ was measured. Regarding these last parameters, that is, G_{ref}, T_{ref} and $I_{sc,ref}$, they generally are empirical values provided by the manufacturer of the panel. As for the constant C_T, it is simply a temperature coefficient that accounts the effect of this variable into the short circuit current.

The diode current, on the other hand, can be expressed by:

$$I_d = I_o \left(e^{\frac{V_d}{aV_t}} - 1 \right) \tag{3}$$

where I_o is the saturation current of the cell, V_t is the thermal voltage of the PV and a is a factor which depends on the doping of the silicon used in the panel [4]. Different from I_o and a, which are constants provided by the manufacturer in the data-sheet, V_t is computed by means of the following formula:

$$V_t = \frac{kT}{q} \tag{4}$$

where k is the Boltzmann constant, 1.38×10^{-23} J/K and q is the electron charge, 1.6×10^{-19} C. The main data of the panel considered throughout this work is summarized in Table 1.

Table 1. Parameters of the used panel

Parameter	Symbol	Value
Referential radiance	G_{ref}	1000 W/m^2
Referential temperature	T_{ref}	298.15 K (25 °C)
Short-circuit current	$I_{sh,ref}$	3.8 A
Saturation current	I_o	2.16×10^{-8} A
Diode coefficient	a	1.12
Thermal constant	C_T	0.0024 A/K
Rated power	–	60.53 W
Rated voltage	–	17.04 V
Number of cells	–	36

Considering the PV panel, for which the technical parameters are presented in Table 1, one may find out the I-V and P-V characteristic curves displayed in Fig. 2. The dots highlighted on the curves indicates either maximum power or current in which the maximum power is achieved. It is possible to notice from Figs. 2(b) and (d) that changes in the radiance and, more significantly, in the temperature which the panel is submitted shifts the voltage in which the maximum power point is achieved.

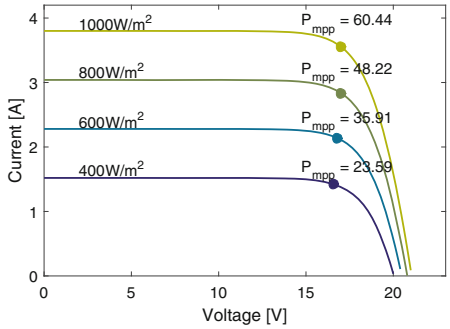

(a) I-V curve under constant temperature

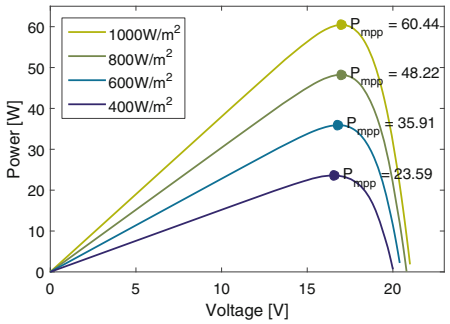

(b) P-V curve under constant temperature

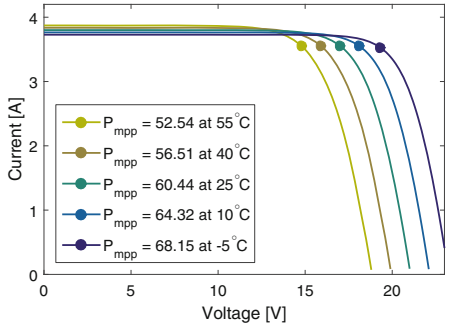

(c) I-V curve under constant radiance

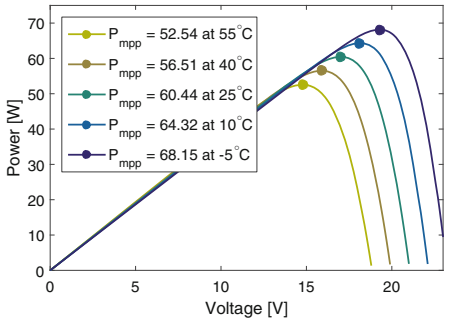

(d) P-V curve under constant radiance

Fig. 2. I-V and P-V curves of a PV panel. (a) and (b) presents the I-V and P-V curves for different values of radiance keeping temperature constant at 25 °C. (c) and (d) presents the I-V and P-V curves for different values of temperature keeping radiance level at 1000 $\mathrm{W/m^2}$.

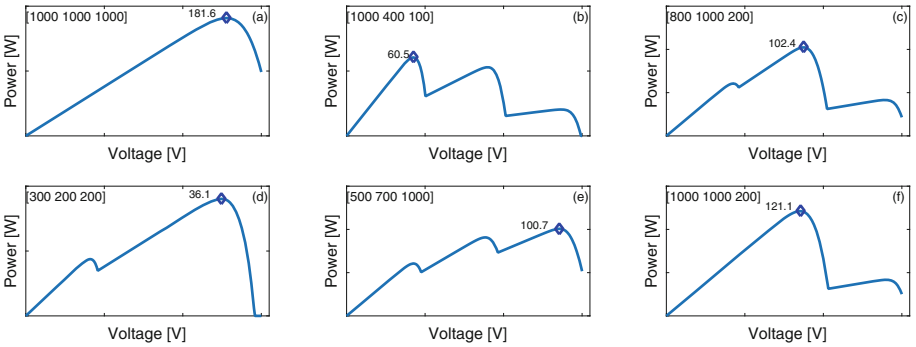

Fig. 3. P-V curve shapes for an array of three series-connected panels under partial shading. The vector $[G_1\ G_2\ G_3]$, placed on each upper left corner, represents the radiance distribution in the panels for that case and the diamond-shaped mark spot the GMPP.

2.2 Characteristics of the PV Panel Under Partial Shading Condition - PSC

The partial shading occurs when an PV panel or an array of panels is submitted to non-homogeneous distribution of radiance. It means that, due to some external factors such as clouds, leaves or even birds and others animals covering part of the panels, the radiance received by part of the cells of a panel is different from the others. In this situation, either cells or even full panels turn into loads for those associated to them, which requires the use of bypass diodes for enhancing power generation [17]. Nonetheless, the result of having panels bypassed when under PSC is that of changing the characteristic of the P-V curve of the group, making room for multiple maximum points as illustrated in Fig. 3. It must be pointed out that the position of the maximum points and quantity of them depends on factors such as number of cells/panels shaded and unshaded, radiance and temperature. It is also important to realize that the peak value of each maximum not necessarily matches the others and that there is no straightforward rule to determine which maximum point is the greatest. Hence, MPPT algorithms can be trapped into local maxima rather than the global.

3 Proposed Scenario and Methodology

Figure 4 presents the scenario considered for evaluation of the PSO-based MPPT. Basically, an array of three series-connected PV panels is feeding a battery through a boost converter. It is important to notice that an input capacitor, C_{in}, is paralleled with the PV array just on the input of the converter. This capacitor plays an important role in the circuit because it is the storage element responsible to sustain the voltage across the PV array, v_{pv}. It is also important to notice that it is possible to change v_{pv} by means adjusting the duty cycle, d, of the converter. Still on the Fig. 4, the block named *Control Algorithms* contains

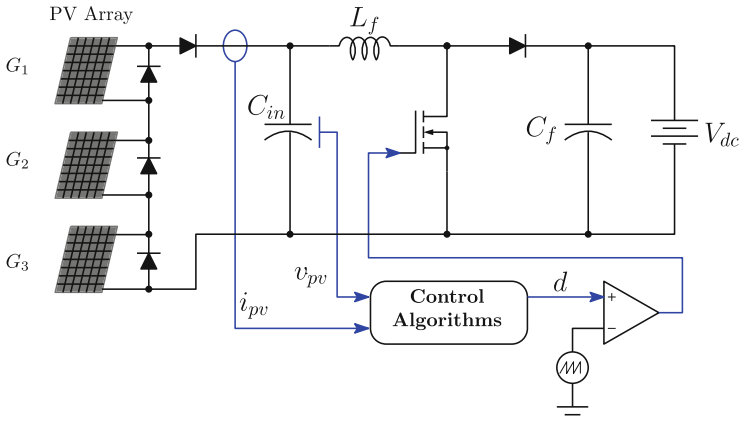

Fig. 4. Reference circuit used throughout the simulations.

the PSO-MPPT algorithm. As it can be seen, both voltage v_{pv} and current i_{pv} of the panels are measured and used to compute the power generated. The output of this block is the duty cycle d which is used to drive the converter. Table 2 presents the parameters used during this paper.

Table 2. Reference for parameters used throughout simulations

Parameter	Symbol	Value
Input capacitance	C_{in}	30 nF
Filter inductance	L_f	0.5 mH
Filter capacitance	C_f	50 µF
Battery voltage	V_{dc}	96 V

4 Particle Swarm Optimization

Basically, the PSO is an AI-based method, similar to genetic algorithms, based on the behavior of flock of birds and others animals [6]. It was observed that the individuals of such groups take advantage of the so call group intelligence to achieve their collective goal, something like finding shelter or food. To cut the long story short, if the objective is to find food, rather than concentrating all the individuals together, the flock is spread over a large area and, as the members communicate with each other, all of them converge to the place which is supposed to have more food available. In the same way, a group of individuals, in this case called particles, is part and parcel of the PSO method. These particles are spread all over the domain of the problem, and they are programmed to gather information and to interact with each other in order to find the solution, which, in general, is the point in the domain which minimizes a previously-established cost function. As the cost function may present local minimum, finding the global inflection point requires well setting of the PSO algorithm, besides the widespread placement of particles.

The PSO algorithm runs on an iterative-approach basis, which means that each particle is initially placed at different spots and, turn after turn, they move around, with changing velocity, towards the solution of the problem [18]. It is important to notice that all spots are mapped on the domain of the problem and, as it has already been stated, the problem itself is to find the minimum point of a user-defined cost function. The velocity u_i with which a certain particle moves is given by:

$$u_i[k] = w\ u_i[k-1] + \underbrace{C_1 r_1 (pbest_i - x[k-1])}_{\text{cognitive component}} + \underbrace{C_2 r_2 (gbest - x[k-1])}_{\text{social component}} \quad (5)$$

where i is the number of the particle, k is the number of the iteration, w is the inertia weight, C_1 and C_2 are positive constants, r_1 and r_2 are random

numbers ranging from 0 to 1, and x is the position of the particle. Besides that, the variables *pbest* and *gbest* correspond to the best positions (positions which returned the best results) achieved, respectively, by this particle and by the whole group, accounting all the previous iterations.

As it can be seen in (5), the velocity of a particle changes with two main parts named cognitive and social. The former is intended to draw upon the particle's own experience, whereas the later focus on the group acquired knowledge. It is worth noticing that the chosen values of the constants C_1 and C_2 are straightforwardly linked with the dynamic of the algorithm and, because of that, these values must be adequately tuned according to the objective. As for the random variables r_1 and r_2, they play an important role in the searching process, avoiding the particles to rapidly settle on an unchanging direction of movement [6]. Other point noteworthy is the role of inertia weight w. The greater this coefficient is, the wider the domain is explored. In other words, bigger values of w promotes better the searching for global minimum of the cost function [18]. Finally, the position of the particle i in the k^{th} iteration is given by:

$$x_i[k] = x_i[k-1] + u_i[k] \tag{6}$$

5 PSO-MPPT

As the voltage across the panels can be controlled by means of changing the duty cycle, d was chosen to be the variable representing the domain of the problem. Thus, the position of each particle, this last being referred as q_i in some graphs, represents a duty cycle and was chosen to be updated as follows:

$$d_i[k] = d_i[k-1] + u_i[k-1] \tag{7}$$

It should be borne in mind that $d_i[k]$ must be bounded within the interval $[0, 1]$, otherwise the PSO algorithm may command a searching outside the domain of the problem. The same way, (5) can be rewritten as:

$$u_i[k] = u_i[k-1] + \underbrace{C_1 r_1 (d_{best,i} - d[k-1])}_{\text{cognitive component}} + \underbrace{C_2 r_2 (d_{best,g} - d[k-1])}_{\text{social component}} \tag{8}$$

where u, in this case, is the rate of change of the duty cycle, which means the velocity of the particle, $d_{best,i}$ and $d_{best,g}$ take the role of *pbest* and *gbest* in (5). Although they are not used in (8) it is important to point that the values of power associated to $d_{best,i}$ and $d_{best,g}$ shall be stored, respectively, in $P_{max,i}$ and $P_{max,g}$. Unfortunately (8) has no bounds and must not be used in this form, otherwise it could threaten the performance of the algorithm. Among different methods for limiting the rate of changing of the duty cycle, it was chosen the trigonometric approach used in [12]. Thus, (8) must be rewritten as:

$$u_i[k] = \frac{2}{\pi} tg^{-1}\Big(w u_i[k-1] + C_1 r_1 (d_{best,i} - d_i[k-1]) + C_2 r_2 (d_{best,g} - d_i[k-1])\Big) \tag{9}$$

since the image of the inverse tangent is $[-\pi/2, \pi/2]$ and it only returns $\pm\pi/2$ in case the argument reaches $\pm\infty$, this formula bounds the velocity within the interval $(-1, 1)$.

When it comes to the cost function, the approach presented in (Sect. 4) was changed according to the current objective—find the MPP. Hence, the algorithm was arranged to search for a maximum instead of a minimum of a function, and this function was considered to be the power produced by the converter.

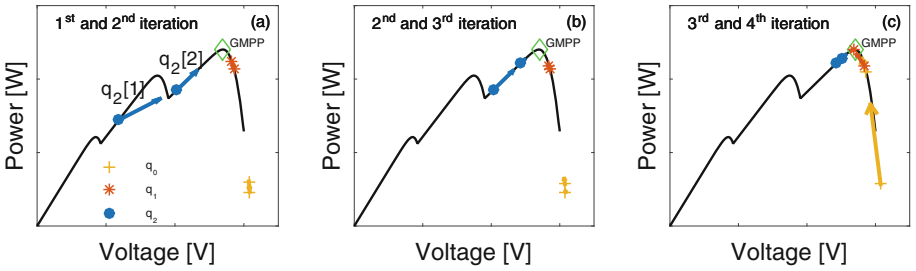

Fig. 5. Particle swarm convergence for three particles, q_0, q_1 and q_2. The size of the arrows are proportional to the velocities and the graphs show the paths from (a) 1st to 2^{nd}, (b) 2^{nd} to 3^{rd}, and (c) 3^{rd} to 4^{th} iterations.

Once explained how the position and velocity of each particle is computed, it is time to present the PSO-MPPT algorithm. Firstly, all particles have to be initialized and this takes an important role in the process. For proper convergence it is necessary not only a certain minimum number of particles, but also that these are properly spread throughout the domain of the problem. To better understand this process, Fig. 5 exemplifies the desired behavior for a case with three particles. In the leftmost square is presented the particles in their initial position, notice that rather than displaying actually the position (duty cycle) it was chosen to spot the point into the P-V curve associated to it. After a couple of turns, the particles move to the positions shown on the central graph and latter on they converge to the global maximum point, as shown in the graph on the right. In order to have a faster and more accurate convergence process it was assigned different ranges for the initialization of each particle. It means that in case we have n particles, their initial position might be a random number within specific intervals, as follows:

$$\begin{aligned} d_1[0] &= rand\left(\left(0, \tfrac{1}{n}\right]\right) \\ d_2[0] &= rand\left(\left(\tfrac{1}{n}, \tfrac{2}{n}\right]\right) \\ &\vdots \\ d_n[0] &= rand\left(\left(\tfrac{n-1}{n}, 1\right]\right) \end{aligned} \tag{10}$$

where $rand()$ is a function which returns a random number within the interval given. This approach guarantee the widespread placement of the particles in the first turn. It was also chosen $u_i[0] = 0$ as initial velocity for each particle.

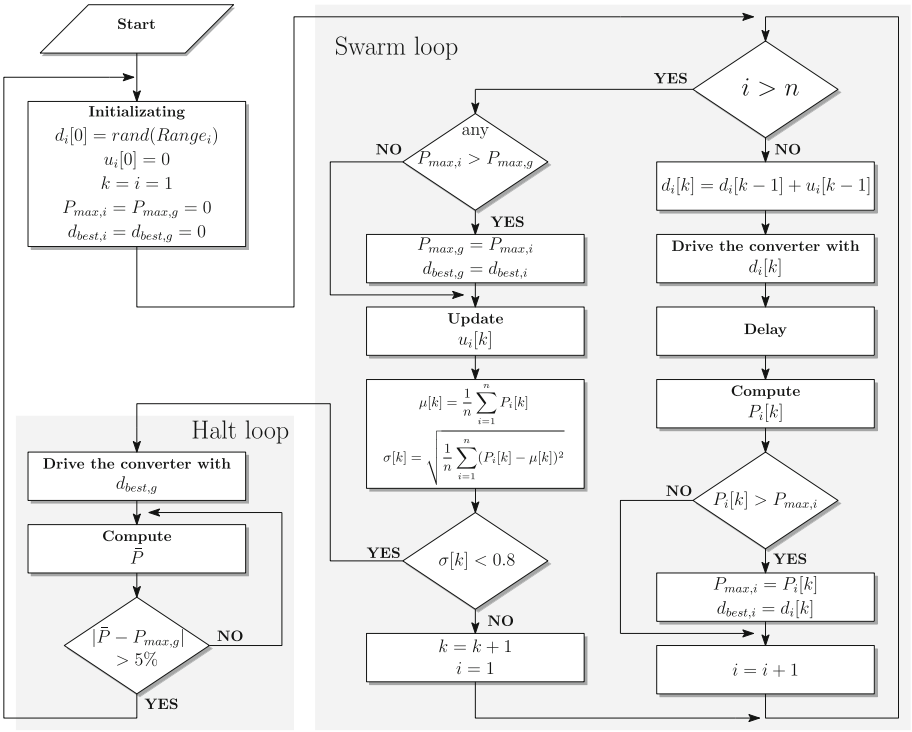

Fig. 6. Particle swarm algorithm flowchart for n particles. The *swarm loop* represents the process of going from particle to particle testing the power response. The *halt loop* goes off whenever the particles converge to GMPP.

After setting the initial states of the particles, the iterative process goes off. In every cycle k, the positions $d_i[k]$ of all n particles are updated according to Eq. (7) and, then, the converter is driven with each value in sequence to compute the generated power $P_i[k]$, from v_{pv} and i_{pv}, associated to each particle. Notice that whenever the duty cycle is changed the circuit undergoes transient state. That is why the measurement of the power is delayed in 4.5 ms. In addition to that, instead of using the instantaneous power, it was chosen to be used the average power computed over 50 samples (covering a period of 0.5 ms) to guarantee that any oscillation or noise in the signals do not compromise the proper work of the algorithm. In case the $P_i[k]$ surpass the maximum power, $P_{max,i}$, achieved by the particle so far, $d_i[k]$ is assigned to $d_{best,i}$, and $P_i[k]$ to $P_{max,i}$. Before finishing the iteration, after all particles have been tested, $P_{max,g}$ and $d_{best,g}$ are updated, case any $P_{max,i}$ surpass its previous value, and the velocities $u_i[k]$ are computed. Attention have to be raised to the fact that even after converging to the MPP, the particles still continue changing position due to the random characteristic of the process and it can cause oscillations on the power generated. Thus, it was chosen to halt the algorithm, and drive the converter with $d_{best,g}$, whenever the

particles crowd each other in a small neighborhood. To infer if the particles are next to each other is used the standard deviation of the average point of $P_i[k]$, given by:

$$\sigma[k] = \sqrt{\frac{1}{n}\sum_{i=1}^{n}(P_i[k] - \mu[k])^2} \tag{11}$$

where

$$\mu[k] = \frac{1}{n}\sum_{i=1}^{n} P_i[k] \tag{12}$$

is the average power of all particles after the k^{th} iteration. The halt loop is commanded to arise whenever $\sigma[k] < 0.8$ is satisfied. The flowchart in Fig. 6 summarizes the algorithm. Notice that once halt, the searching process only restarts if occurs a fluctuation in the generated power $\overline{P}$ bigger than 5%.

6 Methodology and Analysis of Results

This section aims at analyzing the performance of the PSO-MPPT under different setting conditions, it means, different number of particles, values of the constants w, C_1 and C_2. Firstly, it was defined a set of values of the parameters for which the PSO algorithm was to be analyzed. The number of particles, for instance, was set for 3, 5, 7 and 9, on a row, the constants C_1 and C_2, on the other hand, were varied from 1 to 2 with steps of 0.2 and the inertia constant w from 0.2 to 1.0 with the same step size, totaling 720 different combinations of setting points. Considering this space, a set of eight simulations were carried out for each combination to access the performance of the algorithm under different environment conditions. Half of these considered partial shading condition, each one with a different pattern, and the other half full coverage of the sun, with different levels of radiance. The temperature, on the other hand, was held constant at 25 °C for all the aforementioned cases. In summary, it was carried out 5760 simulations, 2880 of which considering partial shading condition. Table 3 summarizes the ranges in which each variable of the simulations were varied.

Table 3. PSO search range parameters

Parameter	Range	Step	Unit
w	$(0.2, 1)$	0.2	–
C_1	$(1, 2)$	0.2	–
C_2	$(1, 2)$	0.2	–
n	$(3, 9)$	2	–
G_1, G_2, G_3	$(400, 1000)$	200	Wm^{-2}
T_{env}	25	0	°C

For the sake of classifying the results, were binarily classified into group A, for those which reached accuracy higher than 99% (virtually 100% accuracy), and group B, for all the other results. In this context, accuracy represents the per unit value of the power produced by the converter taking as reference the theoretical MPP for each case. The global results of simulations and classification are shown in histogram in Fig. 7. As expected, the experiments in scenarios without shading produced virtually 100% accuracy for all the cases. Meanwhile, under partial shading the tests unveiled that only 87.67% (2525) were classified into the group A. Here it is important do state that among those nearly 12% which were classified into the group B, some ended up in a local maxima and others did not converge.

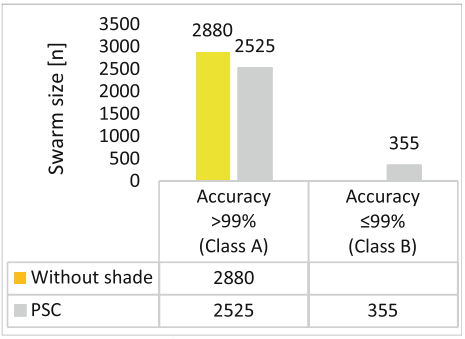

Fig. 7. Accuracy and classification of simulation results independently of the settings

Thenceforth, to compare performance of parameters it was defined the success rate, SR, of the MPPT as follows:

$$SR(i,j,m,l) = \left.\frac{|A|}{|A|+|B|}\right|_{C_1(i),C_2(j),w(m),n(l)} \begin{cases} i,j \in \mathbb{N}^* \mid i,j < 7 \\ m \in \mathbb{N}^* \mid m < 6 \\ l \in \mathbb{N}^* \mid l < 5 \end{cases} \tag{13}$$

Where $|A|$ and $|B|$ represents the number of cases classified in groups A and B for a specific combination or parameters n, C_1, C_2 and w. In short, $SR(i,j,m,l)$ informs the percentage of cases which were classified in the group A for each combination of parameters.

Since the swarm size n is the principal hyper-parameter in the algorithm, we partitioned the SR using this metric. For each number of particles we tested 720 scenarios and the success rate SR for them is shown in Fig. 8. In these graphs, the colors blue and yellow represent the extremities of the results: the lowest and the highest levels of SR. Thus, it was possible to find from Fig. 8(b) that there are 13 combinations of C_1 and C_2 regarding the case with $n = 5$ which the success rate achieved 100%, indicating that all these tests (260) converged

to the GMPP. Notice that the inertia constant varies among all these tests and it is going to be analyzed in the sequence. Due to the fact that the chart for five particles presented the greatest yellow area amongst all, it was decided that the best tracking performance is achieved with $n = 5$.

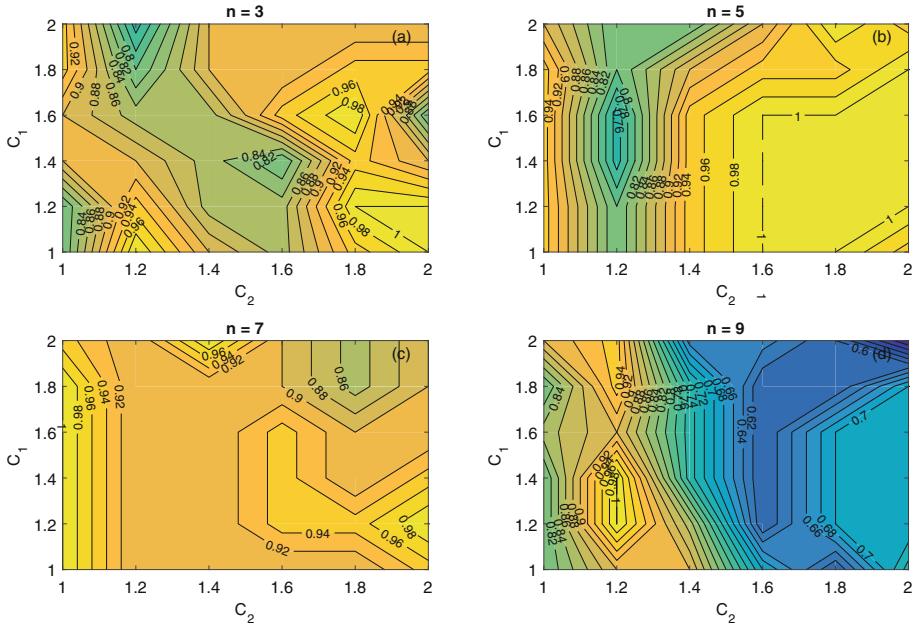

Fig. 8. Success rate mapping for different number of particles (a) $n = 3$: 5 pairs with $SR = 100\%$. (b) $n = 5$: 13 pairs with $SR = 100\%$. (c) $n = 7$: 7 pairs with $SR = 100\%$. (d) $n = 9$: 2 pairs with $SR = 100\%$. (Color figure online)

Considering the 260 successful cases, it means, those detailed in the previous paragraph ($n = 5$), it was analyzed the average convergence time and the results presented in the Table 4. It is observed that the average time grows with the value of the inertia constant w. This happens because, once w goes bigger, the velocity of the particles tends to significantly increase and, thus, the particles jump around the GMPP, leading the PSO algorithm into a larger settling time. It is noticeable, as well, that there is an optimum region on the domain C_1–C_2, represented in Table 4(a) by dashed cells. In this region, the tracking process reaches its lowest value, 0.251 s. It is important to notice that the bounding technique used in (9) is responsible for making different values of C_1 and C_2 produce the same settling time.

In summary, the best results were achieved when swarm size was set for five particles, the constants for cognitive and social components C_1 and C_2 were both set for 1.6, and the inertia weight w for 0.2.

Table 4. Average time in seconds to reach GMPP for class A with size $n = 5$, partitioned by w. The parameters C_1 and C_2 already identified are in boldface inside the dashed cells.

w = 0.2 (a)

C_2 \ C_1	1	1.2	1.4	1.6	1.8	2
1	0.345	0.471	0.439	0.408	0.439	0.377
1.2	0.251	0.251	0.251	0.251	0.251	**0.251**
1.4	0.251	0.251	0.251	0.251	0.251	**0.251**
1.6	**0.251**	**0.251**	**0.251**	**0.251**	0.251	**0.251**
1.8	**0.251**	**0.251**	**0.251**	**0.283**	0.283	**0.314**
2	0.251	0.251	0.251	0.251	**0.251**	0.251

w = 0.4 (b)

C_2 \ C_1	1	1.2	1.4	1.6	1.8	2
1	0.283	0.314	0.314	0.314	0.283	0.283
1.2	0.911	0.251	0.314	0.314	0.314	**0.314**
1.4	0.251	0.251	0.251	0.314	0.314	**0.345**
1.6	**0.377**	**0.377**	**0.377**	**0.408**	1.003	**0.377**
1.8	**0.345**	**0.314**	**0.314**	**0.377**	0.377	**0.377**
2	0.377	0.377	0.345	0.377	**0.439**	0.377

w = 0.6 (c)

C_2 \ C_1	1	1.2	1.4	1.6	1.8	2
1	0.314	0.283	0.345	0.377	0.377	0.377
1.2	0.377	0.544	0.377	0.314	0.377	**0.377**
1.4	0.418	0.418	0.418	0.418	0.418	**0.377**
1.6	**0.377**	**0.377**	**0.345**	**0.345**	0.377	**0.408**
1.8	**0.439**	**0.377**	**0.408**	**0.439**	0.439	**0.408**
2	0.439	0.439	0.439	0.408	**0.408**	0.533

w = 0.8 (d)

C_2 \ C_1	1	1.2	1.4	1.6	1.8	2
1	0.418	0.377	0.418	0.418	0.377	0.439
1.2	0.408	0.377	0.439	0.408	0.377	**0.439**
1.4	0.533	0.533	0.565	0.533	0.460	**0.439**
1.6	**0.502**	**0.439**	**0.439**	**0.471**	0.460	**0.533**
1.8	**0.533**	**0.565**	**0.502**	**0.659**	0.953	**0.596**
2	0.502	0.471	0.471	0.471	**0.471**	0.471

w = 1 (e)

C_2 \ C_1	1	1.2	1.4	1.6	1.8	2
1	0.502	0.502	0.471	0.471	0.502	0.533
1.2	0.502	0.502	0.544	0.585	0.565	**0.565**
1.4	0.502	0.471	0.502	0.533	0.565	**0.502**
1.6	**0.502**	**0.471**	**0.471**	**0.502**	0.502	**0.533**
1.8	**0.502**	**0.502**	**0.471**	**0.439**	0.533	**0.565**
2	0.533	0.471	0.502	0.558	**0.502**	0.621

Figure 9 shows the convergence process observed in the best scenario addressed in the simulation and Fig. 10 shows the search domain. It is highlighted in Fig. 9(c) the final value of $d_{best,g}$ and in (a), the system reached the GMPP at 120 W, for this case. It is possible to notice that it took about 0.25 s, which correspond to 10 swarm cycles, for the system reach to the GMPP. Thus, the hatched areas on the graphs corresponds to the period in which the PSO algorithm was halted for there was not changes into the position of the MPP. These chart also allow us to visualize the heart of the PSO algorithm: the changing values observed in the power and duty cycle shows the algorithm testing the position of each particle on a row, cycle after cycle. Notice that both variables are related to the converter, which means they comprise the results for all the particles of the swarm. As the time moves on, the particles start searching in a

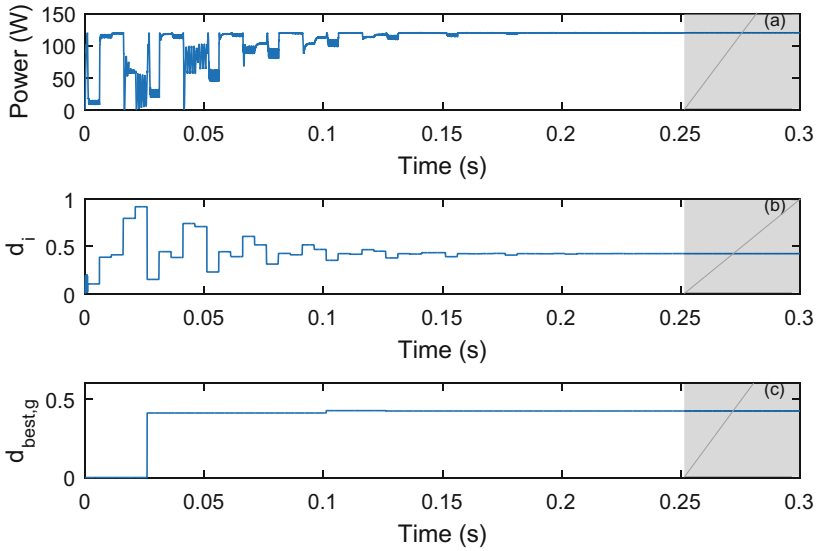

Fig. 9. Convergence process. (a) Output power of PV. (b) Duty cycle. (c) Best duty cycle during search process. After time 0.25 s the search algorithm halts and $d_{best,g}$ is steadily delivered to the power converter.

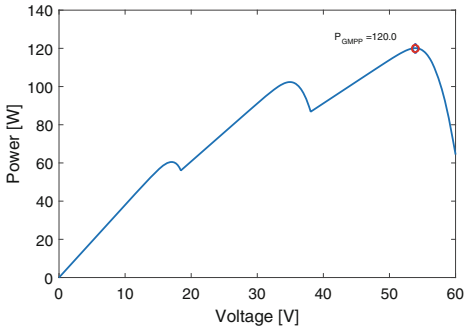

Fig. 10. P-V curve showing the tracked global power point with success rate of 99.9% (best set of parameters found).

narrower neighborhood, which means the difference of duty cycle from particle to particle and from cycle to cycle gradually fade, and eventually they converged to the MPP. It is also worthwhile noticing that $d_{best,g}$ is only changed twice and this results comes from the widespread placement of the particles during the initialization process.

7 Conclusions

This paper presented a general review of the use of PSO in MPPT and the influence of the adjustment of parameters into the performance of the MPP tracking. In a nutshell, it has been presented a grid search over a space of 5760 scenarios for the best combination of parameters, number of particles, C_1, C_2 and w, for the proposed algorithm. From the results, it was possible to conclude that the algorithm is effective and reached the GMPP in almost 88% of proposed cases independently of the settings (number of particles and chosen values for C_1, C_2 and w). It was also noticed that the rate of non-convergence, which in fact, for this analysis, means not reaching the GMPP before $t = 3\,\text{s}$, was low with only 39 out of 5760 cases reporting this behavior. Of course, the algorithm was able to reach the GMPP nearly 100% of the cases for $n = 5$, $C_1 = C_2 = 1.6$ (best setting arrangement). It was also spotted that the best performances, when it comes to the convergence time, led the algorithm to reach GMPP in about 0.25 s.

Besides that, it is also possible to draw some conclusions about the relationship between parameter adjustment and tracking performance:

- Swarm size (n): large number of particles leads to a slower convergence time.
- Inertia coefficient (w): larger value can slow the convergence time since it might require more cycles for all particles get closer to the GMPP.
- Cognitive and social components: inside the algorithm C_1 and C_2 contributes either for local and global maximum searching.

One last point to be made concerns the effect of the general configuration on the results achieved. Since in the present analysis was considered only cases with one, two or three local maxima, it is not possible to guarantee that the performance will be the same for the cases where more than three maxima occurs.

References

1. Arantegui, R.L., Jäger-Waldau, A.: Photovoltaics and wind status in the European Union after the Paris agreement. Renew. Sustain. Energy Rev. **81**, 2460–2471 (2018). https://doi.org/10.1016/j.rser.2017.06.052
2. Bendib, B., Belmili, H., Krim, F.: A survey of the most used MPPT methods: conventional and advanced algorithms applied for photovoltaic systems. Renew. Sustain. Energy Rev. **45**, 637–648 (2015). https://doi.org/10.1016/j.rser.2015.02.009
3. Dolara, A., Leva, S., Manzolini, G.: Comparison of different physical models for PV power output prediction. Sol. Energy **119**, 83–99 (2015). https://doi.org/10.1016/j.solener.2015.06.017
4. Hasan, M., Parida, S.: An overview of solar photovoltaic panel modeling based on analytical and experimental viewpoint. Renew. Sustain. Energy Rev. **60**, 75–83 (2016). https://doi.org/10.1016/j.rser.2016.01.087

5. Ishaque, K., Salam, Z., Amjad, M., Mekhilef, S.: An improved particle swarm optimization (PSO)-based MPPT for PV with reduced steady-state oscillation. IEEE Trans. Power Electron. **27**(8), 3627–3638 (2012). https://doi.org/10.1109/TPEL.2012.2185713
6. Kennedy, J., Eberhart, R.: Particle swarm optimization. In: Proceedings of ICNN 1995 - International Conference on Neural Networks, vol. 4, pp. 1942–1948, November 1995. https://doi.org/10.1109/ICNN.1995.488968
7. Khare, A., Rangnekar, S.: A review of particle swarm optimization and its applications in solar photovoltaic system. Appl. Soft Comput. **13**(5), 2997–3006 (2013). https://doi.org/10.1016/j.asoc.2012.11.033
8. Koad, R.B., Zobaa, A.F., El-Shahat, A.: A novel MPPT algorithm based on particle swarm optimization for photovoltaic systems. IEEE Trans. Sustain. Energy **8**(2), 468–476 (2017). https://doi.org/10.1109/TSTE.2016.2606421
9. Liu, F., Kang, Y., Zhang, Y., Duan, S.: Comparison of P&O and hill climbing MPPT methods for grid-connected PV converter. In: 2008 3rd IEEE Conference on Industrial Electronics and Applications, pp. 804–807, June 2008. https://doi.org/10.1109/ICIEA.2008.4582626
10. Liu, L., Meng, X., Liu, C.: A review of maximum power point tracking methods of PV power system at uniform and partial shading. Renew. Sustain. Energy Rev. **53**, 1500–1507 (2016). https://doi.org/10.1016/j.rser.2015.09.065
11. Malinowski, M., Leon, J.I., Abu-Rub, H.: Solar photovoltaic and thermal energy systems: current technology and future trends. Proc. IEEE **105**(11), 2132–2146 (2017). https://doi.org/10.1109/JPROC.2017.2690343
12. Mirhassani, S.M., Golroodbari, S.Z.M., Golroodbari, S.M.M., Mekhilef, S.: An improved particle swarm optimization based maximum power point tracking strategy with variable sampling time. Int. J. Electr. Power Energy Syst. **64**, 761–770 (2015). https://doi.org/10.1016/j.ijepes.2014.07.074
13. de Oliveira, F.M., da Silva, S.A.O., Durand, F.R., Sampaio, L.P., Bacon, V.D., Campanhol, L.B.: Grid-tied photovoltaic system based on PSO MPPT technique with active power line conditioning. IET Power Electron. **9**(6), 1180–1191 (2016). https://doi.org/10.1049/iet-pel.2015.0655
14. Renaudineau, H., et al.: A PSO-based global MPPT technique for distributed PV power generation. IEEE Trans. Ind. Electron. **62**(2), 1047–1058 (2015). https://doi.org/10.1109/TIE.2014.2336600
15. Rodriguez, E.A., Freitas, C.M., Bellar, M.D., Monteiro, L.F.C.: MPPT algorithm for PV array connected to a hybrid generation system. In: 2015 IEEE 24th International Symposium on Industrial Electronics (ISIE), pp. 1115–1120, June 2015. https://doi.org/10.1109/ISIE.2015.7281628
16. Sen, T., Pragallapati, N., Agarwal, V., Kumar, R.: Global maximum power point tracking of PV arrays under partial shading conditions using a modified particle velocity-based PSO technique. IET Renew. Power Gener. **12**, 555–564 (2018). https://doi.org/10.1049/iet-rpg.2016.0838
17. Shepard, N.: Diodes in photovoltaic modules and arrays. Final report, prepared for JPL by General Electric Company Advanced Energy Systems and Technology Division, King of Prussia, Pennsylvania, 15 March 1984
18. Song, M.P., Gu, G.C.: Research on particle swarm optimization: a review. In: Proceedings of 2004 International Conference on Machine Learning and Cybernetics (IEEE Cat. No.04EX826), vol. 4, pp. 2236–2241, August 2004. https://doi.org/10.1109/ICMLC.2004.1382171

19. Villalva, M.G., Gazoli, J.R., Filho, E.R.: Comprehensive approach to modeling and simulation of photovoltaic arrays. IEEE Trans. Power Electron. **24**(5), 1198–1208 (2009). https://doi.org/10.1109/TPEL.2009.2013862
20. Yu, H.J.J., Popiolek, N., Geoffron, P.: Solar photovoltaic energy policy and globalization: a multiperspective approach with case studies of Germany, Japan and China. Prog. Photovolt. Res. Appl. **24**(4), 458–476 (2014). https://doi.org/10.1002/pip.2560. https://onlinelibrary.wiley.com/doi/abs/10.1002/pip.2560